DOI: 10.30511/pcdp.2025.2063057.1028 - ISSN: 3060-8376 - Vol 2(3), 2025

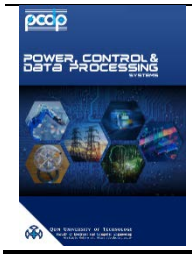

POWER, CONTROL AND DATA PROCESSING SYSTEMS

Available Online at: https://pcdp.qut.ac.ir/

Simulation and Characterization of Multi-Junction Solar Cells with Perovskite/Silicon Absorbers

ARTICLE INFO

Article Type
Original Research

Authors
Tahereh Tavakoli[1, *]
Alireza Mohaghegh Hazrati[2]
Javad Beheshtian[3]

[1] Department of Chemistry, Shahid Rajaee Teacher Training University
elitavakoli991@gmail.com
[2] Department of Physics, K. N. Toosi University of Technology
arm.hazrati@adinra.com
[3] Department of Chemistry, Shahid Rajaee Teacher Training University
j.beheshtian@sru.ac.ir

**** Correspondence***
Address: Department of Chemistry
Shahid Rajaee Teacher Training University.
Phone: -
Fax: -
elitavakoli991@gmail.com

Article History
Received: June 09, 2025
Accepted: August 02, 2025
ePublished: September 01, 2025

ABSTRACT

As global demand for sustainable energy continues to rise, research into photovoltaic technologies has accelerated significantly. However, the presence of toxic lead in conventional perovskite solar cells poses serious environmental and regulatory challenges, impeding large-scale commercialization. To address this issue, this study investigates the replacement of the conventional $CH_3NH_3PbI_3$ absorber with the non-toxic $CH_3NH_3GeI_3$ in a perovskite/silicon tandem configuration. The proposed device, structured as FTO / TiO_2/ $CH_3NH_3GeI_3$ / c-Si(n) / c-Si(p) / c-Si(p^+), was numerically simulated using SCAPS-1D software. Simulation outcomes indicate enhanced performance, achieving a power conversion efficiency (PCE) of 28.98%, short-circuit current density (Jsc) of 43.51 mA/cm², open-circuit voltage (Voc) of 0.78 V, and fill factor (FF) of 85.10%. These findings confirm the potential of $CH_3NH_3GeI_3$ as an eco-friendly and high-performing replacement for lead-based absorbers in tandem solar cell applications, yielding a 0.9% absolute increase in PCE over the reference lead-containing cell.

Keywords: Silicon solar cell, Perovskite solar cell, multi-junction solar cell, SCAPS simulation software.

1 Introduction

The increasing urgency to transition toward clean energy has catalyzed significant advancements in solar photovoltaic (PV) technologies. Among the various configurations, perovskite/silicon tandem architectures stand out for their efficient utilization of a wider solar spectrum, achieved by integrating a wide-bandgap perovskite layer atop a narrow-bandgap silicon base. This architectural synergy enhances light harvesting and may outperform the fundamental efficiency boundary of silicon-only architectures [1], [2].

Despite their high efficiency and rapid development, mainstream perovskite absorbers such as $CH_3NH_3PbI_3$ raise major environmental and health concerns owing to the inclusion of toxic lead. This issue significantly limits their commercial applicability and contravenes global environmental safety standards [3], [4]. Consequently, extensive research has shifted toward the development of lead-free perovskite alternatives that retain high photovoltaic performance while eliminating ecological risks [5].

In response to this challenge, the current study explores the use of $CH_3NH_3GeI_3$ as a lead-free perovskite absorber in tandem solar cell configurations. $CH_3NH_3GeI_3$ exhibits a suitable direct bandgap (~1.9 eV), strong absorption coefficient (>10^5 cm^{-1}), and improved thermal stability compared to its tin-based counterparts, making it a viable candidate for replacing lead-based perovskites in photovoltaic applications [4], [5], [6].

Moreover, silicon remains the dominant material in the PV market due to its abundance, reliability, and mature fabrication infrastructure. With a bandgap of approximately 1.12 eV, crystalline silicon (c-Si) efficiently absorbs the NIR spectral region, which synergistically extends the absorption range beyond what perovskites capture in the visible domain. Therefore, integrating $CH_3NH_3GeI_3$ with c-Si in a tandem architecture provides a strategic pathway for developing next-generation high-efficiency solar cells [1], [7].

This study employs numerical simulation using SCAPS-1D to assess the performance of a tandem solar cell incorporating $CH_3NH_3GeI_3$ as the top absorber. The objective is to evaluate whether the lead-free configuration can match or exceed the performance of traditional $CH_3NH_3PbI_3$-based designs while offering superior environmental compatibility [2], [8].

With the integration of solar cells and smart energy management systems, households can significantly reduce electricity costs. By storing solar energy and utilizing it during periods of peak electricity demand, consumers can optimize energy usage and manage their electricity expenses more efficiently [9].

In recent years, tandem solar cells utilizing perovskite/silicon absorber layers have demonstrated remarkable improvements in power conversion efficiency. Notably, in June 2024, LONGi achieved a record efficiency of 34.6% for this class of solar cells [1], which approaches the theoretical efficiency limit of approximately 45% [8]. These rapid advancements highlight the promising future of perovskite/silicon tandem solar cells in photovoltaic technology.

Compared to other lead-free candidates such as $CH_3NH_3SnI_3$, $CH_3NH_3GeI_3$ shows greater chemical stability and reduced oxidation sensitivity in ambient conditions, making it a more viable replacement in tandem architectures [4], [6]. According to the selected reference article, the baseline device achieved a recorded power conversion efficiency (PCE) of 28.08% [8].

In this study, we aim to optimize this cell by replacing the perovskite absorber layer with a lead-free perovskite material in a silicon/perovskite tandem structure. The optimization and simulation are carried out using the one-dimensional solar cell capacitance simulator (SCAPS-1D) [8].

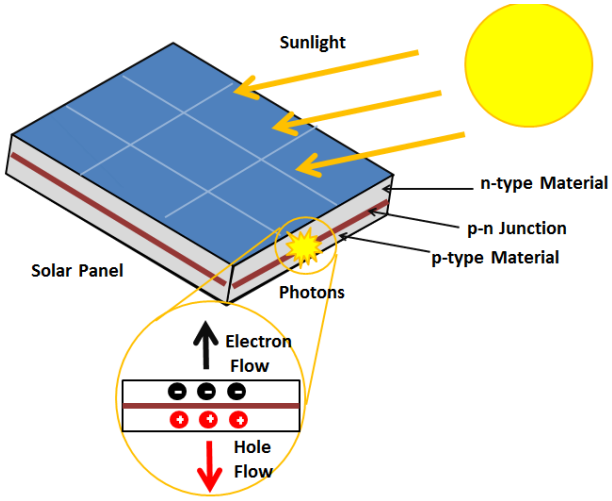

Figure1. Schematic illustration of how a photovoltaic (PV) cell works.

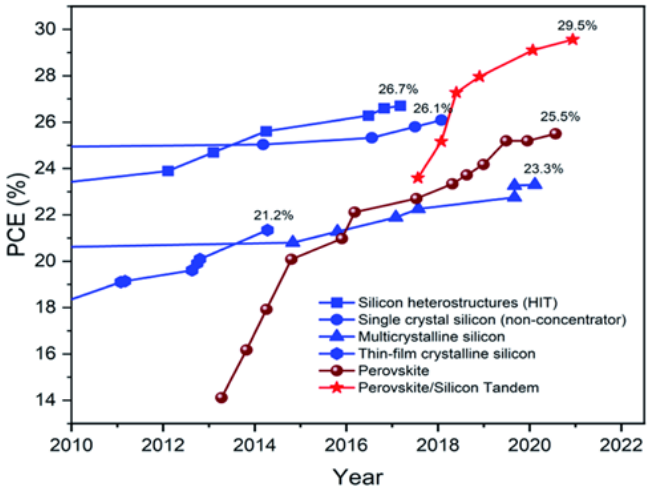

Figure 2. The efficiency of solar cells has increased steadily from the 2010s to 2022, highlighting the superior performance of perovskite/silicon tandem cells compared to monocrystalline silicon cells in recent years.

2 Simulation Method

This investigation utilizes SCAPS-1D, a one-dimensional solar cell simulator developed by the University of Ghent, to

model and evaluate the electrical behavior of the proposed tandem solar cell [10].

SCAPS-1D performs numerical calculations by resolving Poisson's equation alongside electron and hole continuity equations under equilibrium illumination conditions. The tool enables detailed analysis of current–voltage (J–V) characteristics, quantum efficiency (QE), energy band alignment, carrier recombination, and capacitance–voltage (C–V) profiles under standard AM1.5G illumination at 300 K [10].

To ensure that the simulated results emphasize intrinsic material properties, idealized boundary conditions were applied—namely, series resistance (Rs) was set to zero, and shunt resistance (Rsh) was assumed infinite. Parasitic optical losses in the transparent conducting oxide (TCO) layer were also neglected, allowing for a focused assessment of the absorber and adjacent transport layers [2], [8].

The simulator supports up to seven layers, making it well-suited for modeling the complex structure of perovskite/silicon tandem devices [10]. This capability facilitates evaluation of the impact of replacing $CH_3NH_3PbI_3$ with $CH_3NH_3GeI_3$ in the device architecture and provides quantitative insights into the resultant performance enhancements [8], [11].

2.1 Device Structure and Material Properties

The baseline structure used in this simulation is adapted from a previously reported perovskite/silicon tandem configuration featuring a lead-based perovskite absorber. The reference architecture consists of the following layer sequence: FTO / TiO_2/ $CH_3NH_3PbI_3$/ c-Si(n) / c-Si(p) / c $Si(p^+)$. In this design:

- FTO (Fluorine-doped tin oxide) acts as the transparent conducting oxide (TCO), allowing light penetration while conducting photogenerated charges.
- TiO_2 (Titanium dioxide) serves as the electron transport layer (ETL), facilitating efficient electron extraction from the perovskite layer.
- $CH_3NH_3PbI_3$ (Methylammonium lead iodide) is the active light-absorbing perovskite material, responsible for photon absorption and electron–hole pair generation.
- c-Si(n), an n-type crystalline silicon layer, is included to assist in hole transport.
- c-Si(p) serves as the main absorber in the infrared region of the spectrum.
- c-$Si(p^+)$ functions as a back-surface field (BSF), enhancing hole collection and minimizing recombination losses.

The lead-based reference device reported a PCE= 28.08%, J_{sc} = 43.54 mA/cm², V_{oc} = 0.77 V, and FF= 84.74%.

In the modified structure proposed in this study, $CH_3NH_3PbI_3$ is replaced with $CH_3NH_3GeI_3$ to mitigate environmental concerns while retaining performance.

The updated architecture is as follows: FTO/TiO_2/$CH_3NH_3GeI_3$/ c-Si(n) / c-Si(p) / c-$Si(p^+)$.

This new configuration achieved superior photovoltaic metrics in simulation:

- PCE: 28.98%
- J_{sc}: 43.51 mA/cm²
- V_{oc}: 0.78 V
- FF: 85.10%

These results confirm that $CH_3NH_3GeI_3$ not only serves as a safer alternative to lead-based absorbers but also contributes to improved performance outcomes due to its favorable band alignment and reduced recombination at critical interfaces.

2.2 Proposed Solar Cell Structure

In this study, we adopted the same base structure as the reference cell, with one critical modification: the perovskite absorber layer $CH_3NH_3PbI_3$ was replaced with the lead-free compound methylammonium germanium iodide ($CH_3NH_3GeI_3$). This substitution was made to improve both the environmental safety and the overall performance of the device. The modified cell structure is as follows:

FTO / TiO_2/ $CH_3NH_3GeI_3$/ c-Si (n) / c-Si (p) / c-Si (p^+) (Figure 4).

The modified structure achieved:

PCE: 28.98% (+0.9% absolute improvement)
J_{sc}: 43.51 mA/cm²
V_{oc}: 0.78 V
FF: 85.10%

The simulation assumes ideal contact conditions with zero series resistance to isolate material performance. Further, no parasitic absorption was considered in the transparent conductive oxide (TCO) layer.

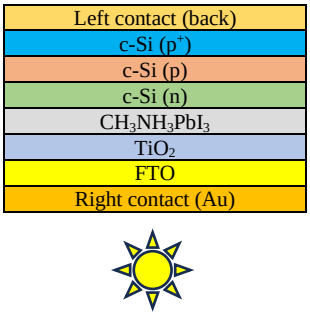

Figure 3. Schematic of the structure of a silicon perovskite solar cell with the structure FTO/TiO_2/$CH_3NH_3PbI_3$/c-Si (n)/c-Si (p)/c-Si (p+)

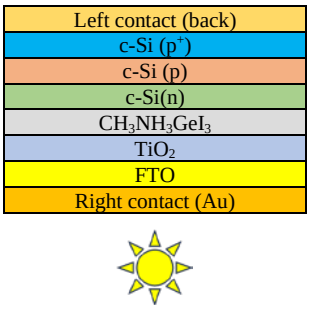

Figure 4. Schematic of the structure of a silicon perovskite solar cell with the structure FTO/TiO_2/$CH_3NH_3GeI_3$/c-Si (n)/c-Si (p)/c-Si (p+)

2.3 Simulation Parameters

The proposed perovskite/silicon solar cell structure was modeled using the SCAPS-1D simulator. The detailed electrical and material properties of all simulated layers are summarized in Table 1. The current–voltage (J–V) characteristics were derived using an equivalent circuit model, with simulations carried out at 300 K under AM1.5G spectral illumination at 1000 mW/cm².

Table 1. Parameters Used in the Simulation

Parameters	FTO	TiO2	CH3NH3GeI3	c-Si(n)	c-Si(p)	c-Si(p++)
Thickness	100nm	50nm	300nm	50nm	100µm	30nm
Acceptor Concentration (cm-3)	0	0	1×1019	0	5×1016	9.5×1018
Donor Concentration (cm-3)	1019	1017	1×1019	8×1016	0	0
Bandgap (ev)	3.5	3.2	1.9	1.124	1.124	1.124
Relative Dielectric Permittivity	9	10	10.00	11.9	11.9	11.9
Electron Mobility (cm2/Vs)	20	20	1.62×105	1250	1010	1212
Hole Mobility (cm2/Vs)	10	10	1.01×105	443	443	421
Electron Affinity (ev)	4	4.0	3.98	3.9	4.05	3.9
Defect Density (cm-3)	1015	1015	2.5×1013	1013	1013	1013
CB effect density of States (cm-3)	2.2×1019	2.2×1019	1×1016	2.8×1019	2.8×1019	2.8×1019
VB effective density of States (cm-3)	1.8×1019	1.8×1019	1 ×1016	1.04×1019	1.04×1019	1.04×1019

2.4 Impact of Perovskite Layer Substitution on J–V Characteristics

The effect of replacing the perovskite absorber layer from $CH_3NH_3PbI_3$ to $CH_3NH_3GeI_3$ on the J–V curve is illustrated in Figure 5 In photovoltaic systems, efficiency is a fundamental indicator that quantifies how effectively a device converts incoming solar energy into electrical power, generally presented as a percentage.

In photovoltaic systems, the generated photocurrent is directly related to the incident light intensity. To achieve high efficiency under specific illumination conditions, a high photocurrent is essential. Under standard test conditions (STC)—with a solar irradiance of 1000 W/m^2 and a temperature of 25° C−the output power of a solar cell is expected to reach its maximum value [12][13].

The simulated J–V curve for both the reference and modified structures is shown in Figure 5, demonstrating the improvement in performance due to the substitution of the perovskite layer.

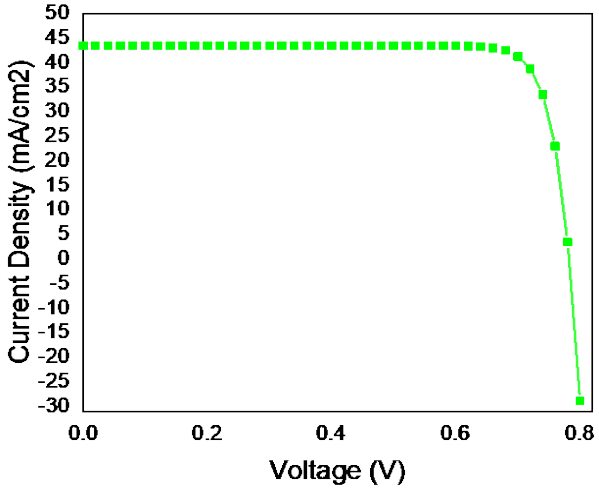

Figure 5. J-V Chart

2.5 Temperature Dependence of Solar Cell Performance

Solar cells are typically installed outdoors, where they operate under continuous sunlight exposure at temperatures exceeding 300 K. Therefore, it is essential to calculate the device performance under varying thermal conditions. The operational temperature of the device is variable and can significantly influence performance metrics.

Figure 6A shows the temperature dependence of the open-circuit voltage (Voc). As expected, Voc decreases with increasing temperature from 300 K to 400 K under different illumination intensities. Notably, the decrease in Voc becomes more pronounced at higher light intensities. This behavior is attributed to the increased intrinsic carrier concentration and reduced built-in potential at elevated temperatures, which adversely affect the balance between generation and recombination processes [11]. The generation rate depends on the solar concentration, absorption, light transmission, and reflection, while the recombination rate is governed by the dominant recombination mechanisms in the perovskite/silicon tandem solar cell structure.

Figure 6B illustrates that the short-circuit current density (Jsc) also decreases significantly as the temperature rises from 300 K to 400 K. Similarly, Figure 6C shows the temperature dependence of the fill factor (FF), which declines with increasing temperature. This drop in FF is primarily linked to the temperature sensitivity of Voc.

In Figure 6D, the variation of power conversion efficiency (PCE) with temperature is presented. For a perovskite/silicon tandem solar cell operating under sunlight, the efficiency drops from 28.88% at 300 K to 21.62% at 400 K. As

Temperature increases, key physical parameters such as electron and hole mobilities and carrier concentrations are affected due to changes in device resistance, ultimately leading to performance degradation. Additionally, the decrease in FF and PCE can be attributed to the reduction in shunt resistance at elevated temperatures.

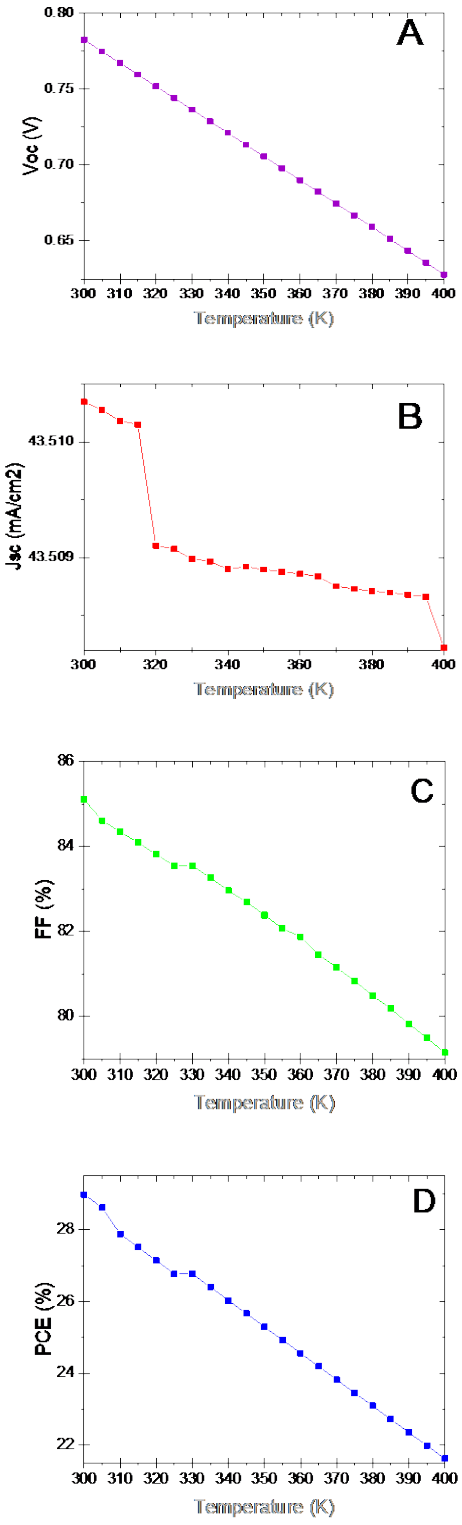

Figure 6. Device Parameter Variations with Temperature:

a) Voc b) Jsc c) FF d) PCE

3 Results and Discussion

3.1 Photovoltaic Performance

The J–V characteristics of the proposed $CH_3NH_3GeI_3$/silicon tandem solar cell demonstrate a power conversion efficiency (PCE) of 28.98%, which surpasses that of the lead-based reference device (28.08%) [8]. The device exhibits a short-circuit current density (Jsc) = 43.51 mA/cm², an open-circuit voltage (Voc) = 0.78 V, and a fill factor (FF) = 85.10%. These enhancements are attributed to improved band alignment at the $TiO_2/CH_3NH_3GeI_3$ interface, higher carrier mobility, and suppressed interface recombination losses, which collectively enhance spectral utilization and reduce energy losses [8], [15].

3.2 Role of c-Si(n) Layer

The n-type crystalline silicon (c-Si(n)) layer acts as a hole transport layer (HTL) in the tandem configuration. This layer facilitates the efficient extraction of holes generated in the perovskite layer and contributes to improved charge transport, which ultimately enhances the current output of the device [8].

3.3 Electron Transport Layer (TiO_2) Functionality

Titanium dioxide (TiO_2) serves as an effective electron transport layer (ETL), enabling electron extraction from the perovskite layer while blocking holes. Its conduction band alignment with $CH_3NH_3GeI_3$ ensures low energy barriers for electron flow and minimizes recombination at the ETL/absorber interface, leading to improvements in Voc and FF [2], [11].**Back Surface Field (c-Si(p^+))**

The heavily doped p^+-type silicon (c-Si(p^+)) layer serves as a back surface field (BSF), reducing recombination losses at the rear contact. It improves hole collection efficiency and enhances carrier lifetime, thereby contributing to an increase in Voc and FF [5], [9].

3.5 Temperature Effects

A thermal stability analysis was performed by simulating device performance at temperatures ranging from 300 K to 400 K. The results indicate a gradual decline in Voc, Jsc, FF, and consequently PCE with rising temperature. Specifically, the PCE drops from 28.88% at 300 K to 21.62% at 400 K. This behavior is consistent with intrinsic semiconductor physics, where elevated temperatures lead to increased recombination, reduced carrier lifetime, and lower mobility [8], [15]. These results highlight the critical importance of implementing thermal management strategies in the practical deployment of tandem solar cells.

4 Conclusion

This study confirms that replacing the lead-based perovskite absorber $CH_3NH_3PbI_3$ with the lead-free alternative $CH_3NH_3GeI_3$ in perovskite/silicon tandem solar cell configurations is a viable and effective strategy to retain high photovoltaic performance while eliminating environmental toxicity [8], [14]. The SCAPS-1D simulation results demonstrate a power conversion efficiency (PCE) of 28.98%, which exceeds the performance of the lead-based reference device (28.08%) [8].

The proposed tandem cell structure—comprising TiO_2 as the electron transport layer (ETL), c-Si(n) as the hole transport layer (HTL), and c-Si(p^+) as the back surface field (BSF)—ensures efficient charge carrier management and minimization of recombination losses, thereby supporting high values of Jsc (43.51 mA/cm²), Voc (0.78 V), and FF (85.10%) [8], [15].

The study further emphasizes the favorable energy band alignment, strong light absorption, and environmental compatibility of $CH_3NH_3GeI_3$, which make a promising absorber material for next-generation solar cells. Moreover, thermal stability analysis reveals that while performance gradually degrades at elevated temperatures, the device maintains competitive efficiency at moderate operating conditions, underlining the importance of thermal management strategies for practical implementation [8], [15].

Finally, replacing toxic lead with environmentally friendly germanium aligns with global safety regulations—such as the European RoHS policy—and contributes to making perovskite/silicon tandem solar technologies more viable for large-scale deployment [14].

Disclosure of Potential Conflicts of Interest

The Authors declare that there is no conflict of interest

Reference

[1] M. A. Green et al., "Solar cell efficiency tables (Version 62)," Prog. Photovolt. Res. Appl., vol. 31, no. 7, pp. 651-663, 2023. DOI: 10.1002/pip.3724.

[2] Rafieipour, P., Mohandes, A., Moaddeli, M., & Kanani, M. (2023). Integrating transfer matrix method into SCAPS-1D for addressing optical losses and per-layer optical properties in perovskite/silicon tandem solar cells. arXiv.

[3] Masoudi, M. R., Haghighi, M., and Rahimipour Behbahani, M., 2024. “Optimal Operation of Solar Energy System Integrated with Energy Storage Systems.” Power, Control, and Data Processing Systems, 1(1), pp. 1–3. DOI: 10.30511/PCDP.2024.718345.

[4] N. K. Noel et al., "Lead-free organic-inorganic tin halide perovskites for photovoltaic applications," Energy Environ. Sci., vol. 7, no. 9, pp. 3061-3068, 2014. DOI: 10.1039/C4EE01076K.

[5] Y. Zhao et al., "Perovskite/silicon tandem solar cells: From fundamental to commercialization," ACS Energy Lett., vol. 6, no. 3, pp. 998-1020, 2021. DOI: 10.1021/acsenergylett.0c02681.

[6] G. E. Eperon et al., "Formamidinium lead trihalide: A broadly tunable perovskite for efficient planar heterojunction solar cells," Energy Environ. Sci., vol. 7, no. 3, pp. 982-988, 2014. DOI: 10.1039/C3EE43822H.

[7] Shi, Y., Berry, J. J., & Zhang, F. (n.d.). Perovskite/silicon tandem solar cells. ACS Energy Letters.

[8] Ghazi, A. N., Khizar, J., Yasir, U., Waqas, M., Saleem, M. K., & Khalid, M. (2021). Numerical modeling and optimization of perovskite silicon tandem solar cell using SCAPS-1D. Scholars Bulletin, 7(7), Article 004.

[9] A. Al-Ashouri et al., "Monolithic perovskite/silicon tandem solar cell with >29% efficiency," Science, vol. 370, no. 6522, pp. 1300-1309, 2020. DOI: 10.1126/science.abd4016.

[10] Hemanan, W. A. (2006). Quantifying global status report. Renewable Energy Policy Network for the 21st Century (REN21).

[11] M. M. Islam et al., "A numerical analysis of lead-free perovskite-based $CH_3NH_3GeI_3$ and $CH_3NH_3SnI_3$ solar cells using SCAPS-1D," Sol. Energy, vol. 206, pp. 522–535, 2020. DOI: 10.1016/j.solener.2020.05.019.

[12] S. Bista et al., "Temperature dependence of perovskite/silicon tandem solar cells," J. Appl. Phys., vol. 128, no. 17, p. 173101, 2020. DOI: 10.1063/5.002505.

[13] M. A. Green, "Solar cell fill factors: General graph and empirical expressions," Solid-State Electron., vol. 24, no. 8, pp. 788–789, 1981. DOI: 10.1016/0038-1101(81)90062-9.

[14] European Commission, "Directive 2011/65/EU on the restriction of the use of certain hazardous substances in electrical and electronic equipment (RoHS)," Off. J. Eur. Union, 2011.

[15] A. Al-Ashouri et al., "Monolithic perovskite/silicon tandem solar cell with >29% efficiency," Science, vol. 370, no. 6522, pp. 1300–1309, 2020. DOI: 10.1126/science.abd4016.